Synthesis and Application of Nano-Al_2O_3 Powder for the Reclamation of Hexavalent Chromium from Aqueous Solutions

Y. C. Sharma,* V. Srivastava, and A. K. Mukherjee

Department of Applied Chemistry, Institute of Technology, Banaras Hindu University, Varanasi-221005, India

The application of nano-Al_2O_3 for the removal of hexavalent chromium has been investigated. The nano-Al_2O_3 was used as an adsorbent in the present study. Nano-alumina was prepared in the laboratory by a sol-gel method. The effect of initial concentration on the removal of Cr(VI) was studied by varying the initial concentration of Cr(VI) from (0.03 to 0.19) mmol·L^{-1}. It was found that the percent removal of Cr(VI) decreases by increasing the initial adsorbate concentration. A contact time of 60 min was found to be sufficient for maximum removal and was recorded as the equilibration time. Resultant data were analyzed by pseudofirst- and pseudosecond-order rate equations. The pH of the solutions affected the removal of Cr(VI) significantly, and removal decreased from (92.2 to 60.8) % by varying the pH from the acidic to alkaline range. Maximum removal was, however, achieved at pH 2.0. It was found that removal decreased by increasing the temperature from (25 to 45) °C. The value of activation energy was very low which indicates that adsorption was physical adsorption. Resulting data at different temperatures were analyzed by the Langmuir and Freundlich equations using linearized equations. Values of different thermodynamic parameters were determined for the resultant data. Values of $\Delta G°$, $\Delta H°$, and $\Delta S°$ were calculated and found to be -4.81 kJ·mol^{-1}, -24.28 kJ·mol^{-1}, and -97.57 kJ·mol^{-1}·K^{-1} at 25 °C at an initial chromium concentration of 0.03 mmol·L^{-1}. Findings of the present study revealed that nano-Al_2O_3 can be an effective adsorbent for the removal of Cr(VI) from aqueous solutions. This study may serve as baseline data and may help in designing wastewater treatment plants for the treatment of Cr(VI) in particular and that for pollutant species in general.

1. Introduction

Water pollution due to the disposal of industrial effluents enriched with toxic metallic species is a matter of concern. Metals have harmful effects on fauna, flora, and human beings. As metals are nonbiodegradable, they have a tendency to accumulate in the environment through the food chain. Cr(VI) is one of the most commonly used metals in the electroplating industry, fertilizers, pigments, tanning, mining, and metallurgical industries.[1] Chromium exists in two stable oxidation states, namely, Cr(III) and Cr(VI).[2] Cr(III) is insoluble in water and essential micronutrient for animals and human beings. It plays an important role in the metabolism of glucose, protein, and lipids. However, Cr(VI) is 500 times more toxic than Cr(III) and known to be carcinogenic and teretogenic.[3,4] It is reported to cause perforation of the nasal septum, renal tubular necrosis, bronchitis, dermatitis, and vomiting. The maximum levels permitted in wastewater are 5 mg·L^{-1} form trivalent chromium and 0.05 mg·L^{-1} for hexavalent chromium.[4]

Various technologies such as chemical precipitation, electrodeposition, reduction, neutralization, reverse osmosis, solvent extraction, ion exchange, and adsorption are available for the removal of metallic pollutants from water and wastewater. That these technologies are related to high maintenance and operational cost, high energy requirements, incomplete metal removal, and the generation of toxic sludge is another major disadvantage related to these techniques.[5,6] Among all methods, adsorption is an economically feasible alternative. Adsorption is versatile method and probably can solve the problem of sludge disposal. Adsorbents can be regenerated and reused which can make the treatment even more cost-effective. A variety of materials like fly ash, moss peat, rice husk, red mud, china clay, wheat bran, iron oxide, activated alumina, sand, zeolite, and so forth have been used as adsorbents for the removal of a variety of pollutants from aqueous solutions and industrial effluents.[7,8]

The application of nanoparticles as adsorbents has come up as an interesting area of research because of their high removal efficiency. Because of their nanosize, these particles have a high surface area and a greater number of active sites to interact with the pollutant species.[9,10] A previous study also indicates that in many cases the adsorption capacity remains almost unchanged after regeneration of the adsorbent, and it could be reused.[11,12] There are various methods for the preparation of nanoparticles such as electrodeposition, mechanical alloying, the sol-gel method, and laser pyrolysis. Among them the sol-gel method has many advantages over the other methods.[13] The sol-gel method is related to the preparation of materials with high purity and homogeneity. Surface properties of the adsorbents can also be modified by the sol-gel method. In present study, nano-Al_2O_3 powder prepared by the sol-gel method was used for the removal of Cr(VI) from aqueous solutions.

2. Experimental Section

2.1. Preparation and Characterization of Nano-Al_2O_3. In the present study, nano-Al_2O_3 powder was prepared by the sol-gel method. For this purpose, low-cost precursor material was used to make the process economically viable. Aluminum sulfate solution was precipitated by ammonia solution for the prepara-

* Corresponding author. E-mail: ysharma.apc@itbhu.ac.in. Tel.: +915426702865. Fax: +91 542 2306428.

10.1021/je900822j
Published on Web 02/16/2010

tion of alumina gel. After drying, the alumina gel was calcined for 1 h in a muffle furnace (Libratherm instrument PID 300 Naskar & Co.) to obtain nano-Al_2O_3. After calcination, powder was characterized by X-ray diffraction (XRD), transmission electron microscopy (TEM), and Fourier transform infrared spectroscopy (FTIR). Phase characterization of calcined powder was conducted by the XRD technique (X-ray diffractometer, Scifert and Co., model ID-3000) using Cu Kα radiation. Crystallite size was determined by using the diffraction peaks from the Scherer formula:[13]

$$X_s = \frac{0.9\lambda}{\mathrm{FWHM}\cos\theta} \quad (1)$$

where X_s = crystallite size (nm), λ = wavelength of monochromatic X-ray beam, $\lambda = 0.154056$ nm for Cu Kα radiation, FWHM = full width at half-maximum for the diffraction peaks under consideration (rad), and θ = diffraction angle (degrees). For the accurate determination of lattice parameters, a database powder diffraction file JCPDS PDF release 1997, International Centre for Diffraction Data (ICCD), was used. The morphology of the powder was determined by using TEM (FEI, Tecani, G^2 20 S-Twin). FTIR spectra of the alumina powder were obtained by using a FTIR spectrometer (Varian 1000 FT-IR, Scimitar Series). FTIR spectra of nanoalumina were recorded between (500 and 4000) cm^{-1}. The samples were ground with 200 mg of KBr in a mortar and pressed into 10 mm diameter disks under 10 tonnes of pressure and high vacuum for FTIR analysis. The Brunauer−Emmett−Teller (BET) surface area of the nano-Al_2O_3 powder was investigated by using a computer controlled automated porosimeter (Micromeritics ASAP 2020, V302G single port). Nitrogen was used as the cold bath (77 K), and classical BET theory was used. The porous structural parameter used in this paper was taken from BJH (Barret−Joyner−Halenda) data. In this study, the powder was evacuated and then cooled to −196 °C using liquid nitrogen before analysis. The adsorption portion of the N_2 isotherm was used to calculate the pore size distribution of nanoalumina particles.

2.2. Adsorption Experiments. The adsorbent nano-Al_2O_3 powder was used for the removal of Cr(VI) from aqueous solutions. Batch adsorption studies were conducted to determine the optimum conditions for the removal of Cr(VI) from aqueous solutions. A stock solution of chromium was prepared by dissolving potassium dichromate in 1000 mL of distilled water, and this solution was used for the preparation of standard and working solutions of various concentrations. The ionic strength of the aqueous solutions was maintained at $1.0 \cdot 10^{-2}$ M $NaClO_4$. The batch adsorption experiments were performed by adding different quantities of nano-Al_2O_3 powder with 50 mL of aqueous solutions of Cr(VI) of varying concentration in 250 mL stoppered conical flasks. All of the adsorption experiments were conducted at 25 °C (± 0.5), the pH of the working solution, and an agitation rate of 100 rpm on a shaking thermostat. After the equilibration time, the adsorbents were separated from the aqueous solutions by centrifugation (Remi 24, New Delhi, India) at 10 000 rpm for 10 min. The residual concentration of Cr(VI) in each aliquot was determined by using a UV−visible spectrophotometer (Bausch and Lomb, USA) at 540 nm with 1,5-diphenyl carbazide following a standard method.[14]

2.3. Chromium(III) Analysis. For the determination of the Cr(III) concentration, Cr(III) (formed due to the reduction of Cr(VI) into Cr(III) during the sorption process) was again converted to Cr(VI) by the addition of excess potassium permanganate at (130 to 140) °C, and 1,5-diphenycarbazide added thereafter. The pink-colored complex formed gives the concentration of Cr(VI) and Cr(III), which is total chromium. The Cr(III) concentration was then calculated by the difference of total chromium and Cr(VI) concentrations. A detailed analysis has been reported by Park et al.[15]

For the purpose, the supernatant liquid (after sorption) was divided into two parts. In one sample, the Cr(VI) concentration (C_e) was measured spectrophotometrically. In contrast, in another sample Cr(VI) was determined after heating the solution up to (130 to 140) °C with $KMnO_4$ solution. It was found that, in both cases, the concentration of Cr(VI) was similar. This analysis confirms that the removal of Cr(VI) by nano-Al_2O_3 was only by the adsorption process. A reduction process was not involved during the removal of Cr(VI) from aqueous solutions. Our findings are supported by those of Park et al.[15]

The amount of Cr(VI) adsorbed per unit mass of the adsorbent was determined by using the following equation:

$$q = (C_i - C_e/W)V \quad (2)$$

where q is the amount adsorbed per unit mass of the adsorbent ($mg \cdot L^{-1}$), C_i and C_e are the initial and equilibrium concentrations of chromium in solution, respectively ($mg \cdot L^{-1}$), W is the mass of the adsorbent (g), and V (L) is the volume of the solution.

The percentage removal of Cr(VI) was calculated by the following equation:

$$\%\ \text{removal of Cr(VI)} = (C_i - C_e)/C_i \cdot 100 \quad (3)$$

3. Results and Discussion

3.1. Characterization of Nano-Al_2O_3 Powder. The formation of alumina in different phases was observed by XRD (Figure 1). Phase analysis was confirmed by their standard patterns. γ and α-alumina phases were present in the synthesized powder. The average crystallite size was determined to be in the range of (15 to 20) nm by using the Scherrer formula. TEM results also support the results of XRD analysis (Figure 2).

The data obtained by BET measurements of nano-Al_2O_3 powder have been given in Table 1. The BET surface area of nano-alumina powder developed at 1100 °C was found to be 78.798 $m^2 \cdot g^{-1}$, whereas the BJH adsorption/desorption surface area of pores was 77.434/84.198 $m^2 \cdot g^{-1}$. The single point total pore volume was found to be 0.40 $cm^3 \cdot g^{-1}$, and the cumulative adsorption/desorption pore volume was 0.39/0.39 $cm^3 \cdot g^{-1}$, respectively. The BJH adsorption/desorption average pore diameter was found to be 206.11/189.31 Å. The porosity and density of the nano-Al_2O_3 powder was determined and found to be 0.51 $g \cdot cm^{-3}$ and 1.33 $g \cdot cm^{-3}$, respectively.

The FTIR spectrum of bare nano-Al_2O_3 powder and chromium-loaded nano-Al_2O_3 powder is shown in Figure 3. The presence of peaks in the region from (3000 to 3600) cm^{-1} are related to the lattice water molecules. It indicates the presence of moisture in the powder or KBr pellet. In the alumina, the vibrations of the OH, Al−OH, and Al−O bonds generated the observed bands in the infrared region. The stretching vibration of the OH ions of residual water and solvent in the gel produced a very intense broad band at (3000 to 3600) cm^{-1} (Figure 3), whereas their bending vibration generated the band at 1632 cm^{-1}.[16] The stretching vibrations of the Al−OH bond gave rise to the band at 1555 cm^{-1}. The weak bands observed between (1100 and 1200) cm^{-1} were produced by Al−O bonds.[16] It is clear from the FTIR figure of the nano-Al_2O_3 powder loaded with Cr(VI) that there is not any significant change in the FTIR of bare and Cr(VI) loaded nano-Al_2O_3 powder, which confirms that there is no formation of new groups between adsorbates and adsorbents.

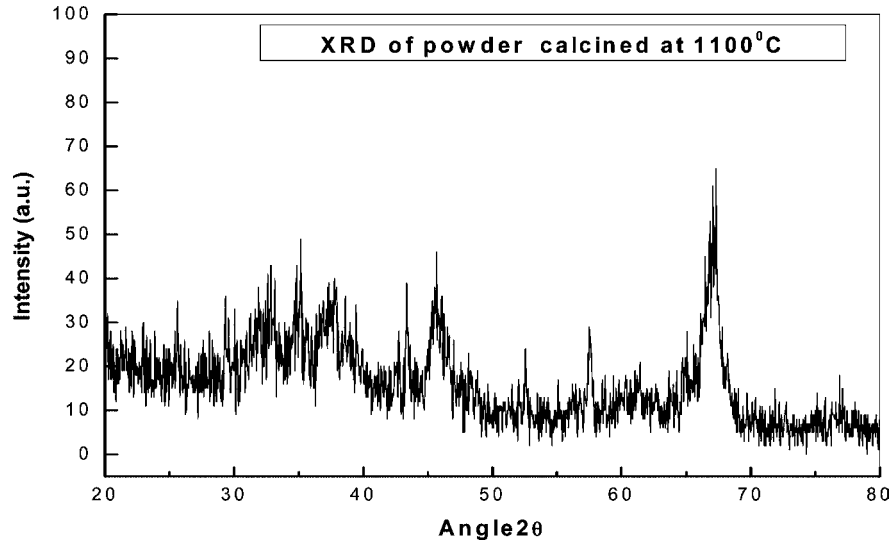

Figure 1. XRD of nano-Al_2O_3 powder.

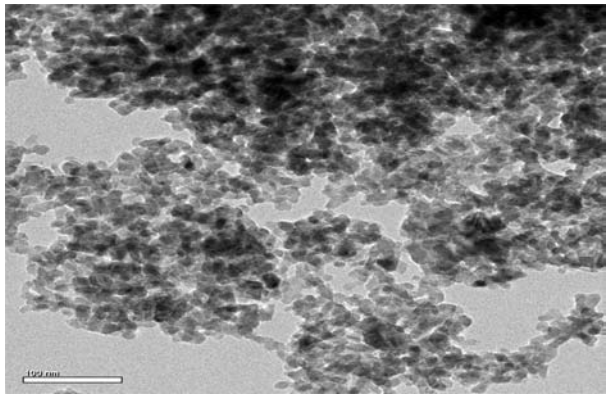

Figure 2. TEM of nano-Al_2O_3 powder.

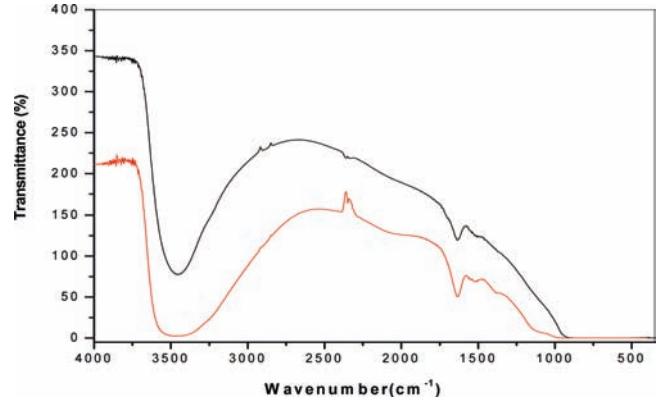

Figure 3. FTIR of bare nano-Al_2O_3 powder and Cr(VI)-loaded nano-Al_2O_3 powder.

Table 1. Results of Brunauer−Emmett−Teller (BET) Measurements for Nano-Al_2O_3

surface area	BET surface area ($m^2 \cdot g^{-1}$)	78.79
	BJH adsorption cumulative surface area of pores ($m^2 \cdot g^{-1}$)	77.43
	BJH desorption cumulative surface area of pores ($m^2 \cdot g^{-1}$)	84.20
pore volume	single point adsorption total pore volume of pores ($cm^3 \cdot g^{-1}$)	0.40
	BJH adsorption cumulative volume of pores ($cm^3 \cdot g^{-1}$)	0.39
	BJH desorption cumulative volume of pores ($cm^3 \cdot g^{-1}$)	0.39
pore size	adsorption average pore width (Å)	204.21
	BJH adsorption average pore diameter (Å)	206.11
	BJH desorption average pore diameter (Å)	189.31

3.2. Effect of Concentration and Contact Time. During the removal of pollutant species from aqueous solutions and effluents, two factors affecting the removal, the initial concentration of the pollutants, and time of contact of the adsorbate and the adsorbent are of significant importance. A rapid transport of the pollutant species from the bulk solution onto the surface of the adsorbent cuts short the time required to attain equilibrium. The time required to attain equilibrium is important to determine the efficiency of the adsorbent materials. The entire surfaces in aqueous solution are naturally charged, and this charge is governed by the time of contact of the adsorbate and adsorbent. Knowledge of the rate and mechanism of the uptake of the adsorbate species is important for understanding adsorbate−adsorbent systems.

For the investigation of the effect of initial concentration and contact time on Cr(VI) removal by nano-Al_2O_3, experiments were conducted in the concentration range of (0.03 to 0.19) $mmol \cdot L^{-1}$ at 25 °C, at $1.0 \cdot 10^{-2}$ M $NaClO_4$ ionic strength and 100 rpm. The effect of initial concentration and contact time on Cr(VI) removal by nano-Al_2O_3 is shown in Figure 4. It is clear from this figure that the removal of Cr(VI) is rapid in the initial stages and becomes slower gradually, and then at the equilibrium stage and thereafter, there is no significant increment in removal. The time of equilibrium was 60 min for the present system. By increasing the initial concentration from (0.03 to 0.19) $mmol \cdot L^{-1}$, the removal decreased from (87.45 to 84.94) %. This period of reaction time was sufficient for maximum removal of Cr(VI) from aqueous solution.

3.3. Effect of Adsorbent Dose. In the present study, the effect of adsorbent dose was studied by changing the amount of adsorbent dose from (2 to 20) $g \cdot L^{-1}$ and keeping other experimental conditions constant. The effect of adsorbent dose on Cr(VI) removal by nano-Al_2O_3 is shown in Figure 5. It is clear from this figure that the removal (%) increased by increasing the adsorbent dose. It can be explained on the basis that increasing the adsorbent dose for a fixed concentration of adsorbate, a larger number of active sites are available which results in increased removal of the chromium species.

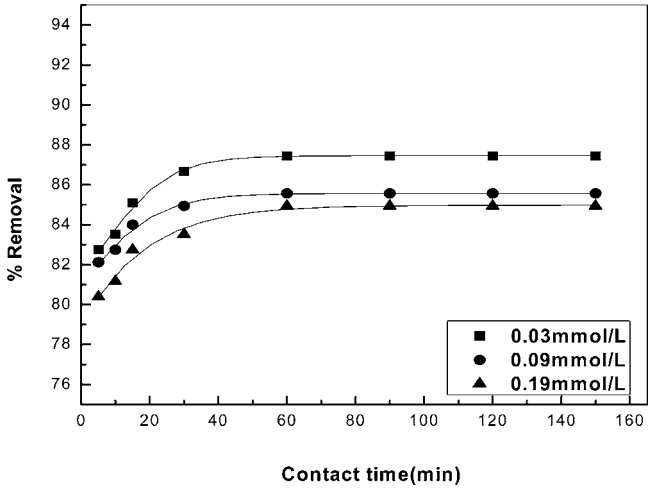

Figure 4. Effect of concentration and contact time on percent removal of Cr(VI) by nano-Al_2O_3 powder.

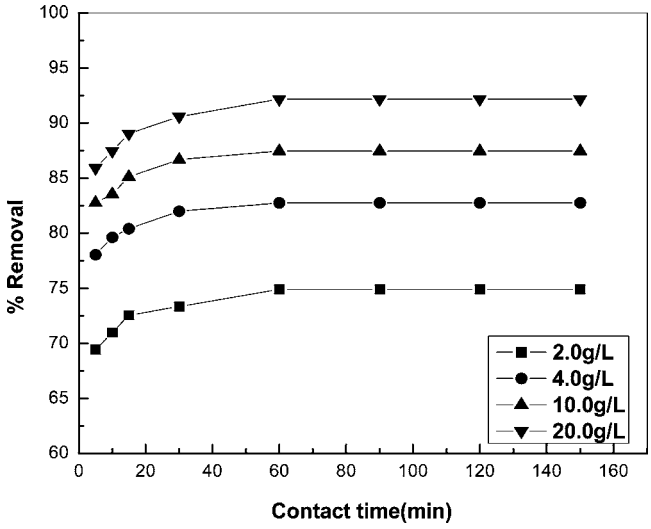

Figure 5. Effect of adsorbent dose on percent removal of Cr(VI) by nano-Al_2O_3.

4. Kinetic Modeling of the Adsorption of Cr(VI) on Nano-Al_2O_3 Powder

Adsorption kinetic models are important in the process of the removal of metals from aqueous solutions. Models of adsorption kinetics correlate with the solute uptake rate, so these models are important in water treatment process design. The study of adsorption kinetics is significant as it provides valuable insight into the reaction pathways and the mechanism of the reactions. Any adsorption process is normally controlled by the three steps: (i) transport of the solute from bulk solution to the film surrounding the adsorbent, (ii) the film to the adsorbent surface, and (iii) the surface to the active sites.

The slowest steps determine the overall rate of the adsorption process, and usually it is thought that step ii leads to surface adsorption and step iii leads to removal through intraparticle diffusion. In the present study, the kinetics of the removal of Cr(VI) was carried out to understand the adsorption behavior of the nano-Al_2O_3 powder. To understand the mechanism of adsorption and potential rate-controlling step, the adsorption kinetics was investigated by using pseudofirst-order and pseudo second-order kinetic equations to test experimental data. Intraparticle diffusion and mass transfer analysis are also undertaken to decipher the mechanism of the removal.

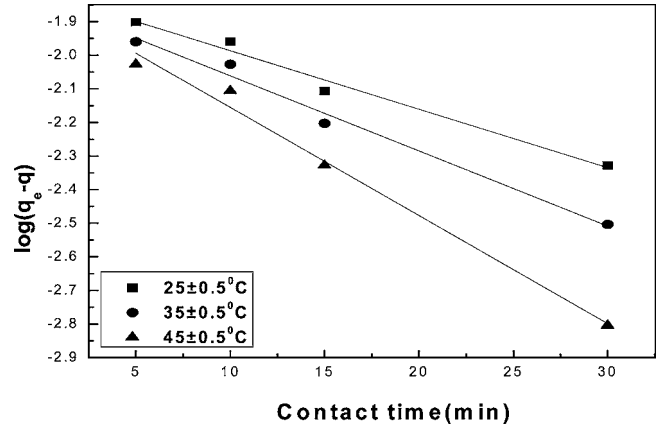

Figure 6. Pseudofirst-order plot for Cr(VI) by nano-Al_2O_3 at different temperatures.

4.1. Pseudofirst-Order Model. The pseudofirst-order model can be expressed by the following equation:[17]

$$\frac{dq}{dt} = k_1(q_e - q_t) \tag{4}$$

where q_e and q_t ($mg \cdot g^{-1}$) are the amounts of adsorbed metallic species on the adsorbent at equilibrium and at time t, respectively. k_1 (min^{-1}) is the rate constant of the first-order kinetic equation. The integrated form of the above equation is as follows:

$$\log q_e = \log(q_e - q_t) - \frac{k_1}{2.303}t \tag{5}$$

The value of k_1 was obtained from the slope of the linear plots of log ($q_e - q_t$) versus t (Figure 6) at different temperatures and q_e from the intercept.

4.1.1. Pseudosecond-Order Model. The adsorption data were also analyzed by a pseudosecond-order kinetic equation. The second-order model can be expressed as follows:[18]

$$\frac{dq}{dt} = k_2(q_e - q_t)^2 \tag{6}$$

where k_2 ($g \cdot (mg \cdot min)^{-1}$) is the rate constant of the pseudo-second-order equation. The integrated form of the above equation can be expressed as follows:

$$\frac{t}{q_t} = \frac{1}{k_2 q_e^{\,2}} + \frac{1}{q_e}t \tag{7}$$

$$h = k_2 q_e^{\,2} \tag{8}$$

where h is the initial sorption rate. The values of q_e and k_2 can be determined by the slope and intercept of the straight line of the plot t/q_t versus t, respectively (Figure 7).

The values of pseudofirst-order and pseudosecond-order rate constants for the removal of Cr(VI) by adsorption on nano-Al_2O_3 at different temperatures were calculated from the straight line plots of Figures 6 and 7, and their values are given in Table 2. The linear plots (Figures 6 and 7) indicate applicability of the kinetic model. The value of the pseudofirst-order constant k_1 decreases by increasing temperature for Cr(VI) adsorption on nano-Al_2O_3 (Table 2). It reveals that higher temperature does not favor the adsorption of Cr(VI) on nano-Al_2O_3 and confirms that the Cr(VI) adsorption on nano-Al_2O_3 is exothermic in nature. Furthermore, the value of calculated q_e from pseudo-second-order kinetics almost agreed with the experimental values of q_e (Table 2). These results indicate that the adsorption of Cr(VI) on nano-Al_2O_3 follows pseudosecond-order kinetics. A

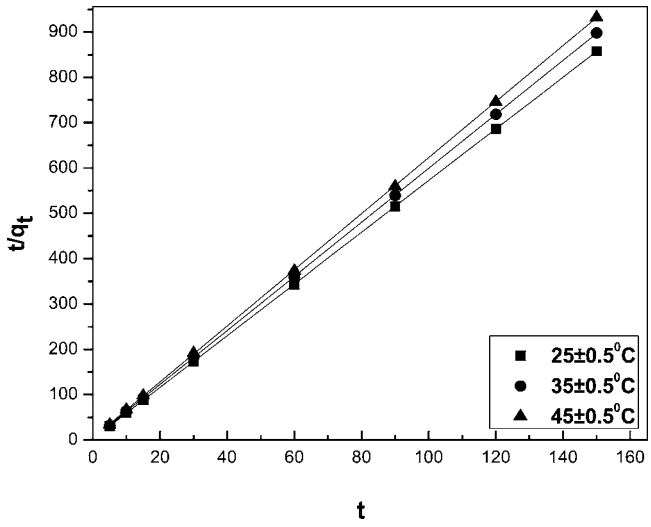

Figure 7. Pseudosecond-order plot for Cr(VI) removal by nano-Al_2O_3 powder at different temperatures.

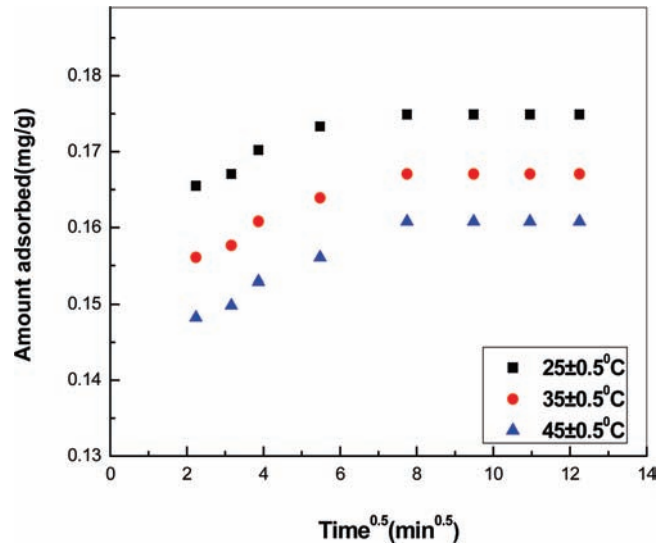

Figure 8. Intraparticle diffusion Cr(VI) by nano-Al_2O_3 powder.

perusal of the values of R^2 clearly indicates that the pseudo-second-order kinetic model better fits the experimental data of the present study. This further supports the validity of this model.

4.1.2. Intraparticle Diffusion Study. The most commonly used technique for identifying the mechanism involved in the sorption process is by fitting the experimental data in an intraparticle diffusion model. The overall adsorption of solute onto the solid surface may be controlled by one or more steps, for example, boundary layer (film) or external diffusion, pore diffusion, surface diffusion, and adsorption onto the pore surface or in combination of several steps. Generally, an adsorption process is diffusion-controlled if the rate is dependent upon the rate of diffusion of the components toward one another. In the usual batch experiments, the adsorption can also occur by intraparticle diffusion.

Further, the porosity of the adsorbent is 0.51, which is quite significant. It has been reported[19] that porous adsorbents exhibit a higher extent of intraparticle diffusion, and the same has been confirmed in the present study.

To confirm this, the value of the rate constants of intraparticle diffusion k_{id} were determined from the slopes of the linear portions of the plots of amount adsorbed versus square root of time at different temperatures by using the following equation[19]

$$q = k_{id}t^{1/2} \tag{9}$$

where q is the amount adsorbed at time t (mg·g^{-1}) and $t^{1/2}$ is the square root of the time (min$^{1/2}$).

It is an empirical functional relationship common to most adsorption processes where uptake varies almost proportionally with $t^{0.5}$ rather than with contact time as such. The values of k_{id} were calculated from the slopes of the curves at different temperatures for intraparticle diffusion (Figure 8). Values of k_{id} at different temperatures are given in Table 3. The graphs of Figure 8 show a dual nature: curved initial portions and linear final portions. This dual nature of the graphs can be attributed to the varying extent of uptake of the adsorbate species initially and in the final stages. In the initial stages, the adsorption occurred because of boundary layer diffusion, and the linear portion indicates uptake because of intraparticle diffusion of the adsorbate.

4.1.3. Mass Transfer Study. For any process of removal by adsorption, it is important to know the extent of transfer of pollutant species from bulk solution to the surface of the solid adsorbent particles and at the interface of solid adsorbent particles or at the interface of liquid and solid particles. A number of steps can be considered participating in the process: (1) the mass transfer of sorbate from the aqueous phase on the solid surface, (2) the sorption of solute on to the surface sites, and (3) the internal diffusion of solute via either a pore diffusion model or homogeneous solid phase diffusion model.

During the present study step 2 has been assumed to be rapid enough with respect to other steps, and therefore it is not rate-limiting in any kinetic study. For the present study this probability was examined by using the following mass transfer model:[20]

$$\ln\left(\frac{C_t}{C_0} - \frac{1}{(1+mk)}\right) = \ln\left(\frac{mk}{1+mk}\right) - \left(\frac{1+mk}{mk}\right)\beta_L S_s t \tag{10}$$

where k is a constant and is the product of Langmuir's parameters, m is the mass of the adsorbent per unit volume, β_L, and the coefficient of mass transfer, S_s, is the specific surface area. The values of m and S_s have been determined as follows:

$$m = \frac{W}{V} \tag{11}$$

$$S_s = \frac{6m}{d_p\delta_p(1-\varepsilon_p)} \tag{12}$$

Table 2. Pseudofirst-Order and Pseudosecond-Order Rate Constants for Cr(VI) Removal by Nano-Al_2O_3 at Different Temperatures

		pseudofirst-order model			pseudosecond-order model		
temperature	experimental values, q_e	k_1	q_e		k_2	q_e	
°C	mg·g^{-1}	min^{-1}	mg·g^{-1}	R^2	g·mg^{-1}·min^{-1}	mg·g^{-1}	R^2
25	0.18	0.07	0.15	0.99	15.44	0.18	1
35	0.17	0.05	0.02	0.98	11.24	0.17	0.999
45	0.16	0.04	0.01	0.98	8.78	0.16	0.999

Table 3. Intraparticle Diffusion Rate Constant at Different Temperatures for Adsorption of Cr(VI)on Nano-Al_2O_3

temperature (0.5 °C)	intraparticle diffusion rate constant K_{id} mg·g^{-1}·min^{-1}
25	0.17
35	0.15
45	0.13

where ε_p is porosity of the adsorbent, d_p is the diameter of the adsorbent, and δ_p is the density of the adsorbent. Values of β_L, the coefficient of mass transfer, were calculated at different temperatures by the slopes and intercepts of the plots of ln [(C_t/C_o − 1/(1 + mk)] versus t (Figure 9), and the values are given in Table 4. A value of β_L of the order of 10^{-5} or greater shows that the rate of transfer of mass from bulk solution to the solid surface is rapid enough.[21] It is clear from the perusal of the plots that some points deviate from linearity. This is because of variation in the extent of mass transfer at those stages. Further, the values of β_L at (25, 30, and 45) °C were of the order of 10^{-6} which suggest that the chances of mass transfer being the rate-controlling step are more.

4.2. Effect of pH on the Removal of Metallic Species from Aqueous Solutions. pH is an important parameter in any adsorption process, and because of its importance it is often quoted as a master variable in removal processes. It strongly affects the removal of metals from aqueous solutions. Variation in pH can strongly affect the surface of the adsorbent and degree of ionization. It is reported that different species of particular ions would be present in a system of that adsorbate. For the effect of pH on percent removal of Cr(VI), the pH range selected was 2.0 to 10.0. The effect of pH on the removal of Cr(VI) by adsorption on nano-Al_2O_3 is given in Figure 10. It is clear from this figure that, when pH increases from 2.0 to 10.0, the removal (%) of Cr(VI) decreases. The removal of Cr(VI) by nano-Al_2O_3 decreases from (92.16 to 60.78) % by varying the pH from the acidic range to the basic range. Similar findings were also reported by other investigators.[22] It may be due to the presence of more H^+ ions at lower values of pH. At lower values of pH, $HCrO_4^-$ is a major species. At lower pH, OH^- groups are neutralized by hydrogen ions, and adsorption of this species is favored. $HCrO_4^-$ is introduced in solution according to following chemical reaction:

$$Cr_2O_7^{2-} + H_2O \rightarrow 2HCrO_4^- \qquad (13)$$

At higher pH, $Cr_2O_7^{2-}$ and CrO_4^{2-} are present in aqueous solution. In this condition the presence of a larger number of OH^- hinders the diffusion of dichromate ions, and therefore the removal percentage of chromium decreases by increasing pH. It is clear from the characterization of the adsorbent that it is an oxide. The oxides of adsorbents undergo surface hydroxylation forming surface hydroxyl compounds. As a result of their subsequent dissociation, these produce negatively or positively charged surfaces as follows:[23]

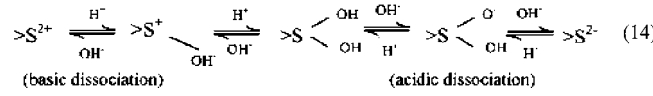

(14)

where S stands for Al. It is clear from the above scheme that, with a decrease in pH of the solution, the positive charge density on the adsorbent surface increases and hence the adsorption of Cr(VI) also increases. A pH of approximately 2.0 will be quite favorable for the removal of the dominating $HCrO_4^-$ species. As the solution pH increases, less functional groups are deprotonated, but also more OH^- ions compete with the coexistence of $HCrO_4^-$ and CrO_4^{2-} ions for the active surface sites. Consequently, it is difficult for them to form complexes, and the adsorbed amount will decrease. Significant adsorption at neutral and negatively charged surfaces, however, cannot be explained on the basis of electrostatic attraction only. Specific chemical interactions and surface complexation have also been suggested to describe the removal of adsorption of Cr(VI) from aqueous solutions and wastewater. The adsorption beyond pH 4.5 will include CrO_4^{2-} ions, and the following surface complexation scheme has been suggested:

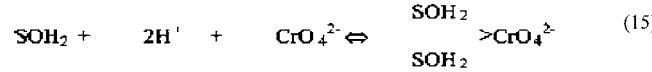

(15)

This type of model has also been reported earlier to explain the adsorption of Cr(VI).[24]

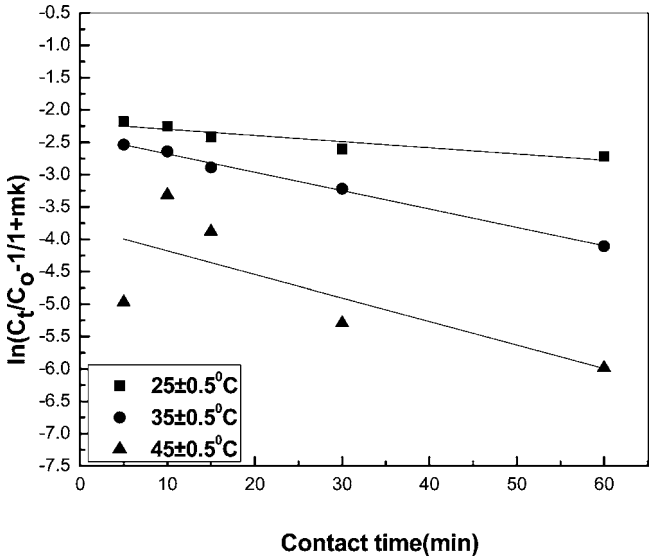

Figure 9. Plot for mass transfer of Cr(VI) by adsorption on nano-Al_2O_3 powder at different temperatures.

Table 4. Values of the Mass Transfer Coefficient for Cr(VI) Adsorption on Nano-Al_2O_3 at Different Temperatures

temperature (0.5 °C)	coefficient of mass transfer, β_L 10^{-6} cms^{-1}
25	0.64
35	0.57
45	0.20

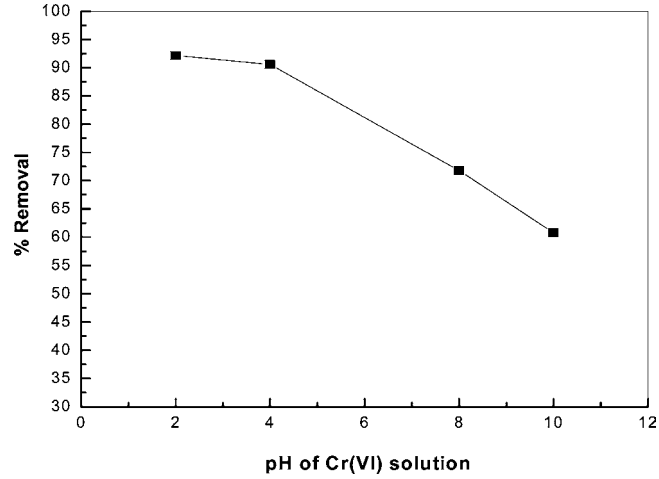

Figure 10. Plot for maximum percent removal of Cr(VI) at different pH values of solutions by nano-Al_2O_3 powder.

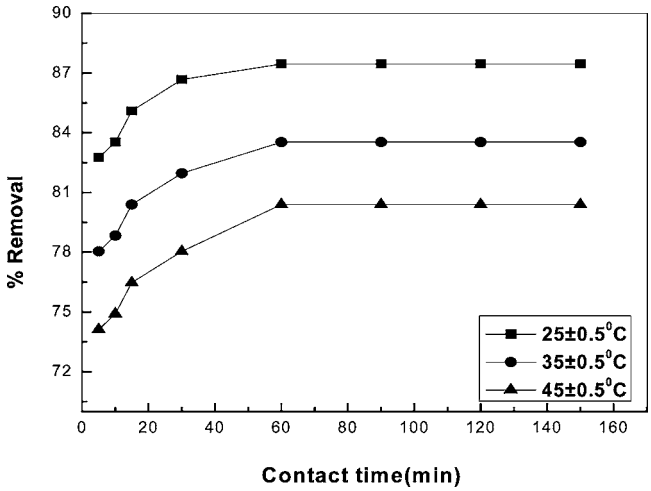

Figure 11. Effect of temperature on percent removal of Cr(VI) from aqueous solutions by nano-Al_2O_3 powder.

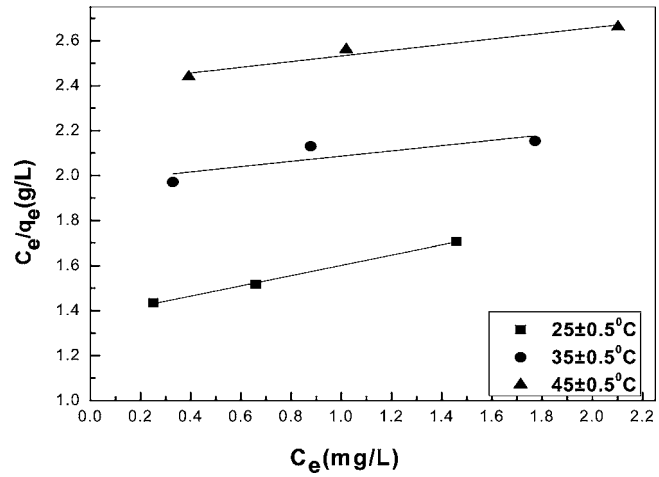

Figure 12. Langmuir plots for the removal of Cr(VI) by adsorption on nano-Al_2O_3 powder.

4.3. Effect of Temperature. Temperature is an important parameter affecting adsorption processes. Most of the adsorption processes are exothermic in nature, but in some cases endothermic adsorption is reported.[2] In the present investigation, the adsorption of Cr(VI) by nano-Al_2O_3 was investigated at the temperatures [25, 35, and 45 (± 5)] °C. The results of the effect of temperature on the adsorption of Cr(VI) on nano-Al_2O_3 are shown in Figure 11. It was found that the percent removal decreases from (87.45 to 80.39) % by increasing temperature from (25 to 45) °C. It indicates that adsorption is exothermic in nature. Lower values of temperature were found to be favorable for Cr(VI) removal from aqueous solutions. The exothermic nature of Cr(VI) adsorption on riverbed sand has also been reported.[25] Further, the variation in the removal of chromium by nanoalumina can be attributed to the enhancement of the relative escaping tendency of the adsorbate species from the solid phase to the bulk phase and a reduction in boundary layer thickness as shown in Figure 8.

4.4. Activation Energy of Cr(VI) Removal by Nano-Al_2O_3 Powder. The activation energy E_a can be calculated by using the Arrhenius equation:[26]

$$\ln k_1 = \ln A - E_a/RT \tag{16}$$

where A is the pre-exponential factor, k_1 the rate constant for the metal adsorption, E_a the activation energy in kJ·mol^{-1}, T the temperature (K), and R the gas constant (8.314 kJ·mol^{-1}·K^{-1}). The value of E_a was calculated by a graphical method and found to be 17.75 kJ·mol^{-1}. From the plot of ln k versus 1/T plot, the pre-exponential factors were calculated to be 986, 734, 588, and 437 for pH 2.0, 4.0, 8.0, and 10.0, respectively. The values of A suggested that the rate of adsorption would increase at increasing temperature and a lower value of pH. The apparent activation energies were found to be (74.20, 72.86, and 67.84) kJ·mol^{-1} for 2.0, 4.0, 6.0, and 8.0 pH, respectively. The magnitude of activation energy also suggests whether or not the uptake of the adsorbate is governed by physical adsorption, and in the case where values of activation energy are in the range of (39.71 to 399.20) kJ·mol^{-1}, uptake is governed by chemical adsorption. The values of E_a ranging from (67.84 to 74.20) kJ·mol^{-1} for the present study suggest that the uptake is controlled by physical adsorption.

4.5. Equilibrium Modeling. Equilibrium studies for any process of removal are of immense importance, especially to recommend the process for large-scale application. Equilibrium modeling of the removal process at different temperatures was carried out considering the Langmuir and Freundlich isotherm models.

4.5.1. Langmuir Adsorption Isotherm. The Langmuir adsorption model is based on monolayer coverage of the adsorbent. The Langmuir isotherm is based on the assumption that maximum adsorption corresponds to a saturated monolayer of solute molecules on the adsorbent surface, that the energy of adsorption is constant. The linearized expression of the Langmuir model can be expressed as follows:[13]

$$\frac{C_e}{q_e} = \frac{1}{Q^0 b} + \frac{C_e}{Q^0} \tag{17}$$

where C_e (mg·L^{-1}) and q_e (mg·g^{-1}) are the concentrations of adsorbate and amount of adsorbate adsorbed at equilibrium, respectively. Q^0 (mg·g^{-1}) and b (L·mg^{-1}) are the terms related to capacity and energy of adsorption, respectively, and are known as Langmuir's constants. The equilibrium data were plotted for C_e/q_e versus C_e (Figure 12).

For the Langmuir isotherm, a dimensionless separation factor can be expressed by the following equation:[27]

$$R_L = \frac{1}{(1 + bC_0)} \tag{18}$$

where C_0 is the initial concentration (mg·L^{-1}) and b is the Langmuir adsorption equilibrium constant (L·mg^{-1}). The dimensionless constant separation factor, R_L, is used to test whether the adsorption is favorable or not. The values of R_L indicate the type of the isotherm to be either unfavorable ($R_L > 1$), linear ($R_L = 1$), favorable ($0 < R_L < 1$), or irreversible ($R_L = 0$).

Langmuir capacities were calculated by using eq 17. The equilibrium data have been plotted for Cr(VI)-nano-Al_2O_3 as C_e/q_e versus C_e (Figure 12). It is clear from the figures that all of the graphs are single, smooth, and continuous. This nature of the graphs indicates that the removal of the metallic species is culminated through a monolyer coverage on the surface of the selected nanoadsorbent.

The value of the two Langmuir's constants, Q^0 and b, were determined by the slopes and intercepts of the related figures. The calculated values of Q^0 and b at different temperatures have been given in Table 5. The value of R_L is tabulated in Table 6. It is clear from Table 5 that values of Q^0 decrease with increasing temperature. A decreasing trend of Q^0 with temper-

Table 5. Values of Langmuir and Freundlich Constants for Adsorption of Cr(VI) by Nano-Al_2O_3

	Langmuir constants			Freundlich constants		
temperature	Q^0	b		K_f	b	
(0.5 °C)	mg·g^{-1}	L·mg^{-1}	R^2	mg·g^{-1}	L·mg^{-1}	R^2
25	8.56	0.18	0.96	0.58	1.14	0.99
35	7.94	0.06	0.73	0.47	1.06	0.99
45	3.95	0.05	0.83	0.39	1.04	0.99

Table 6. Dimensionless Constant Separation Factor R_L for Cr(VI) Removal by Nano-Al_2O_3 at Different Temperatures of Cr(VI) Solutions

temperature	
(0.5 °C)	R_L
25	0.055
35	0.059
45	0.124

ature further confirms involvement of an exothermic process for the removal of chromium. The linear plots of Figure 12 in the concentration range studied confirm the validity of the above model for the present system. The validity of the Langmuir model is further confirmed by values of R_L. For all of the systems the value of R_L is $(0 < R_L < 1)$, which suggests that the Langmuir isotherm is favorable for all of the systems (Table 6).

4.5.2. Freundlich Adsorption Isotherm. The equilibrium data were also examined by the Freundlich isotherm. The Freundlich model assumes that the uptake of metal ions occurs on a heterogeneous adsorbent surface. The Freundlich equation indicates the adsorptive capacity or loading factor on the adsorbent surface and is expressed as follows:

$$q_e = K_f C^{1/n} \tag{19}$$

The logarithmic form of the equation is expressed as follows:[13]

$$\log q_e = \log K_f + \frac{1}{n \log C_e} \tag{20}$$

where K_f is the Freundlich constant denoting adsorption capacity (mg·g^{-1}) and n is the empirical constant indicating adsorption intensity (L·mg^{-1}), which depends on the temperature and properties of adsorbate and adsorbent.

They are a measure of adsorption capacity of adsorbent and adsorption intensity, respectively. C_e is the residual concentration of solute remaining in the solution (mg·L^{-1}), and q_e is the amount of adsorbate adsorbed by a unit mass of adsorbent at equilibrium (mg·g^{-1}). The value of K_f and $1/n$ are calculated by the slopes and intercepts of the plots of log C_e versus log q_e (Figure 13). The values of the constants K_f and n, determined from Figure 13, have been given in Table 5. Linear plots confirm the applicability of the Freundlich isotherm for the undertaken systems. It is clear from Table 5 that the values of K_f decrease with increasing temperature. This is due to the exothermic nature of the adsorption process. On the basis of comparisons of R^2 values for both the Langmuir and the Freundlich adsorption isotherms, it can be concluded that the Cr(VI)-nano-Al_2O_3 system can be better explained by the Freundlich adsorption isotherm than the Langmuir isotherm.

4.5.3. Thermodynamic Studies. Thermodynamic studies were undertaken to elucidate the mechanism involved in the process of removal of Cr(VI) by adsorption on nano-Al_2O_3. Values of thermodynamic parameters were calculated at different temperatures from (25 to 45) °C to investigate the adsorption mechanism of Cr(VI) on nano-Al_2O_3. The following thermodynamic parameters, namely, variation of free energy ($\Delta G°$), enthalpy ($\Delta H°$), and entropy ($\Delta S°$) were determined by using the following expressions:[13]

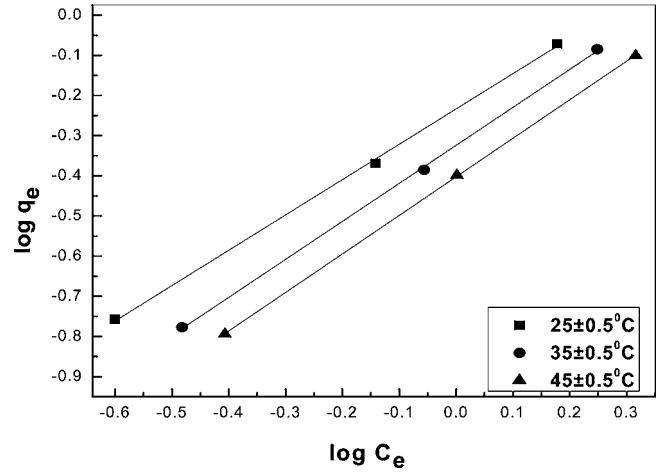

Figure 13. Freundlich plots for the removal of Cr(VI) by adsorption on nano-Al_2O_3 powder.

Table 7. Values of Various Thermodynamic Parameters for Removal of Cr(VI) by Nano-Al_2O_3 Powder

temperature	$\Delta G°$	$\Delta H°$	$\Delta S°$
K	kJ·mol^{-1}	kJ·mol^{-1}	J·mol^{-1}·K^{-1}
298	−4.81	−24.24	−97.44
308	− 4.14		
318	− 3.72		

$$\Delta G^o = -RT \ln K_c \tag{21}$$

$$K_c = C_{ac}/C_e \tag{22}$$

where K_c is the equilibrium constant, C_{ac} and C_e are the equilibrium concentrations of Cr(VI) on the adsorbent and equilibrium concentration of metallic ions in the solution, respectively (mg·L^{-1}), R is the gas constant (1.987 cal·mol^{-1}·K^{-1}), and T is the absolute temperature (K). K_{c1} and K_{c2} are the equilibrium concentrations at T_1 and T_2

$$\Delta H^0 = R\left(\frac{T_2 T_1}{T_2 - T_1}\right) \ln \frac{K_{c2}}{K_{c1}} \tag{23}$$

$$\Delta S^0 = \frac{(\Delta H^0 - \Delta G^0)}{T} \tag{24}$$

Values of these parameters are given in Table 7. For the adsorption of Cr(VI), the values of $\Delta G°$ are negative, which indicate that the adsorption process is spontaneous. The value of the enthalpy change $\Delta H°$ was found to be negative for this system which confirms the exothermic nature of the process of adsorption. Negative values of entropy confirm the possibility of favorable adsorption.

5. Comparative Study of the Adsorption Capacity of Nano-Al_2O_3 and Conventional Adsorbents

Apparently, the adsorption capacity of the adsorbent selected for the present studies is quite comparable with those reported in Table 8. A comparison of the maximum adsorption capacity, Q^0, of the nano-Al_2O_3 with those of the other low-cost adsorbents reported in the literature is given in Table 8. The adsorption capacity of nano-Al_2O_3 is relatively low when compared with activated charcoal; however, it is higher than the other adsorbents reported, namely, activated rice husk carbon, activated alumina, river bed sand, fly ash, saw dust, and so forth (Table 8).

Table 8. Adsorption Capacities of Different Adsorbents for Cr(VI)

adsorbents	adsorption capacity $mg \cdot g^{-1}$	ref
maple waste	5.1	28
bagasse	0.03	29
flyash	0.01	29
wollastonite	0.52	30
waste tea	1.55	31
activated rice husk carbon	0.8	32
activated alumina	1.6	32
soya cake	0.28	33
cactus	7.08	34
activated charcoal	12.87	33
river bed sand	0.15	25
sawdust	0.229	35
nano-Al_2O_3	8.563	present study

6. Summary

On the basis of the results the following conclusions may be drawn:

1. Nano-Al_2O_3 powder can be successfully used for Cr(VI) removal from aqueous solutions.

2. The sol-gel process adopted for the preparation of nanoadsorbent is simple and economically viable because of the use of low-cost precursors.

3. Higher removal was achieved in the acidic range, that is, at pH 2.0.

4. The adsorption of Cr(VI) on nano-Al_2O_3 was found to be exothermic in nature.

5. The process of removal was governed by pseudosecond-order kinetics.

6. The kinetic and equilibrium modeling parameters can be used to design treatment plants for the treatment of Cr(VI)-rich wastewater.

7. Thermodynamic parameters revealed that the removal process is spontaneous and also confirms the exothermic nature of the removal process.

The value of the adsorption capacity of nano-Al_2O_3 was found to be significant, which indicates that it can be successfully used for the removal of Cr(VI). These studies may serve as baseline data and may help in designing wastewater treatment plants for the treatment of Cr(VI) in particular and for pollutant species in general.

Literature Cited

(1) Bansal, M.; Garg, U.; Singh, D.; Garg, V. K. Removal of Cr(VI) from aqueous solutions using pre-consumer processing agricultural waste: A case study of rice husk. *J. Hazard. Mater.* **2009**, *162*, 312–320.

(2) Sharma, Y. C.; Uma; Srivastava, V.; Srivastava, J.; Mahto, M. Reclamation of Cr(VI) rich water and wastewater by wollastonite. *Chem. Eng. J.* **2007**, *127*, 151–156.

(3) Bhattacharya, A. K.; Naiya, T. K.; Mandal, S. N.; Das, S. K. Adsorption, kinetics and equilibrium studies on removal of Cr(VI) from aqueous solutions using different low-cost adsorbents. *Chem. Eng. J.* **2008**, *137*, 3.

(4) Acar, F. N.; Malkoc, E. The removal of chromium(VI) from aqueous solutions by Fagus orientalis L. *Bioresour. Technol.* **2004**, *94*, 13–15.

(5) Suksabye, P.; Thiravetyan, P.; Nakbanpote, W. Column study of chromium(VI) adsorption from electroplating industry by coconut coir pith. *J. Hazard. Mater.* **2008**, *160*, 56–62.

(6) Monteagudo, J. M.; Ortiz, M. J. Removal of Inorganic Mercury from Mine Wastewater by Ion-Exchange. *J. Chem. Technol. Biotechnol.* **2000**, *75*, 767–772.

(7) Baral, S. S.; Das, S. N.; Rath, P.; Chaudhury, G. R. Chromium(VI) removal by calcined bauxite. *Biochem. Eng. J.* **2007**, *34*, 69–75.

(8) Ayuso, E. A.; Sanchez, A. G.; Querol, X. Adsorption of Cr(VI) from synthetic solutions and electroplating wastewaters on amorphous aluminium oxide. *J. Hazard. Mater.* **2007**, *142*, 191–198.

(9) Khaleel, A.; Kapoor, P. N.; Klabunde, K. J. Nanocrystalline metal oxides as new adsorbents for air purification. *Nanostruct. Mater.* **1999**, *11*, 459–468.

(10) Hristovski, K.; Baumgardner, A.; Westerhoff, P. Selecting metal oxide nanomaterials for arsenic removal in fixed bed columns: From nanopowders to aggregated nanoparticle media. *J. Hazard. Mater.* **2007**, *147*, 265–274.

(11) Hu, J.; Lo, I. M. C.; Chen, G. H. Fast removal and recovery of Cr(VI) using surface modified jacobsite($MnFe_2O_4$) nanoparticles. *Langmuir* **2005**, *21*, 11173–11179.

(12) Hu, J.; Chen, G.; Lo, I. C. M. Selective removal of heavy metals from industrial wastewater using maghemite nanoparticles: Performance and mechanisms. *J. Environ. Eng. Div. (Am. Soc. Civ. Eng.)* **2006**, 709–715.

(13) Sharma, Y. C.; Srivastava, V.; Upadhyay, S. N.; Weng, C. H. Alumina Nanoparticles for the Removal of Ni(II) from aqueous Solutions. *Ind. Eng. Chem. Res.* **2008**, *47*, 8095–8100.

(14) *APHA Standard methods for the examination of water and wastewater*, 14th ed.; APHA, AWWA: Washington, DC, 1985.

(15) Park, D.; Yun, Y. S.; Park, J. M. Reductio of hexavalent chromium with the brown seaweed Ecklonia biomass. *Environ. Sci. Technol.* **2004**, *38*, 4860–4864.

(16) Vazquez, A.; Lopez, T.; Gomez, R.; Bokhimi, M.; Novarot, O. J. X-Ray Diffraction, FTIR, and NMR characterization of Sol-Gel Alumina Doped with Lanthanum and Cerium. *Solid State Chem.* **1997**, *128*, 161–168.

(17) Malkoc, E. Ni(II) removal from aqueous solutions using cone biomass of Thuja orientalis. *J. Hazard. Mater.* **2006**, *137*, 899–908.

(18) Ho, Y. S.; Mckay, G. Sorption of dyes and copper ions on to adsorbents. *Process Biochem. (Oxford, U.K.)* **2003**, *38*, 1047–1061.

(19) Weber, W. J.; Morris, J. C.; Sanit, J. *Eng. Div. Proc. Anal. Soc. Civil Eng. 89 (SA2)* **1963**, *31*, 28s.

(20) McKay, G.; Otterburn, M. S.; Sweeny, A. G. Surface mass transfer process during colour removal from effluents using silica. *Water Res.* **1981**, *15*, 321–331.

(21) Gupta, G. S.; Prasad, G.; Singh, V. N. Removal of colour from wastewater by sorption for water reuse. *J. Environ. Sci. Health* **1988**, *A23*, 205–218.

(22) Weng, C. H.; Sharma, Y. C.; Chu, S. H. Adsorption of Cr(VI) from aqueous solutions by spent activated clay. *J. Hazard. Mater.* **2008**, *155*, 65–75.

(23) Ahmed, S. M. Studies of the dissociation of oxides surfaces at the liquid-solid interface. *Can. J. Chem.* **1966**, *44*, 1663–1670.

(24) Davis, J. A.; Leckie, J. O. Adsorption of chromium on activated carbons. *J. Colloid Interface Sci.* **1980**, *74*, 32–37.

(25) Sharma, Y. C.; Weng, C. H. Removal of chromium(VI) from water and wastewater by using riverbed sand: kinetic and equilibrium studies. *J. Hazard. Mater.* **2007**, *142*, 449–454.

(26) Aksu, Z. Determination of the equilibrium, kinetic and thermodynamic parameters of the batch biosorption of nickel(II) ions onto Chlorella vulgaris. *Process Biochem. (Oxford, U.K.)* **2002**, *38*, 89–99.

(27) Basha, S.; Murthy, Z. V. P.; Jha, B. Biosorption of hexavalent chromium by chemically modified seaweed, Cystoseira. *Chem. Eng. J.* **2008**, *137*, 480–488.

(28) Yu, L.; Shukla, S.; Dorris, K.; Shukla, A.; Margrave, J. Adsorption of Cr from aqueous solution by maple sawdust. *J. Hazard. Mater.* **2003**, *100*, 53–63.

(29) Rao, M.; Parwate, A. V.; Bhole, A. G. Removal of Cr^{6+} and Ni^{2+} from aqueous solution using bagasse and fly ash. *Waste Manage. (Amsterdam. Neth.)* **2002**, *22*, 821–830.

(30) Sharma, Y. C. Cr(VI) removal from industrial effluents by adsorption on an indigenous low cost material. *Colloid Surf., A* **2003**, *215*, 155–162.

(31) Orhan, Y.; Buyukgungor, H. The removal of heavy metals by using agricultural waste. *Water Sci. Technol.* **1993**, *28*, 247–55.

(32) Bishnoi, N. R.; Bajaj, M.; Sharma, N.; Gupta, A. Adsorption of Cr(VI) on activated rice husk carbon and activated alumina. *Bioresour. Technol.* **2004**, *91*, 305–307.

(33) Daneshvar, N.; Salari, D.; Aber, S. Chromium adsorption and Cr(VI) reduction to trivalent chromium in aqueous solutions by soya cake. *J. Hazard. Mater.* **2002**, *94*, 49–61.

(34) Dakiky, M.; Khamis, M.; Manassra, A.; Mereb, M. Selective adsorption of chromium(VI) in industrial wastewater using low-cost abundantly available adsorbents. *Adv. Environ. Res.* **2002**, *6*, 533–540.

(35) Morshedzadeh, K.; Soheilizadeh, H. R.; Zangoie, S.; Aliabadi, M. *Removal of chromium from aqueous solutions by lignocellulosic solid wastes*, 1st Environment conference, Tehran University, Department of Environment Engineering, 2007.

Received for review October 10, 2009. Accepted February 6, 2010. The authors are thankful to All India Council of Technical Education to carry out this study by providing NDF to Uma.

JE900822J